Underwater Noise Emissions From Bubble Clouds

NAN Q. LU, ANDREA PROSPERETTI, AND SUK WANG YOON, SENIOR MEMBER, IEEE

(Invited Paper)

Abstract—**By means of an effective equation model for the propagation of pressure waves in a bubbly liquid, the normal modes of oscillation of regions of bubbly liquid in an otherwise pure liquid are calculated for some simple geometries. It is shown that the frequencies of oscillation of such bubble clouds can be very much lower than those of the constituent bubbles in isolation and fall well within the range where substantial wind-dependent noise is observed in the ocean. A comparison with some experimental data very strongly supports the theoretical results.**

I. Introduction

In the ocean, bubble clouds are incessantly formed in the upper layers by the breaking of waves and are transported to depths of tens of meters by Langmuir circulation, turbulence, and other mechanisms [1], [2]. One might expect these bubbles to contribute substantially to the underwater ambient noise, since wave breaking is a catastrophic event that will certainly impart them an appreciable initial energy [3]–[7]. That a substantial part of this acoustic emission could be at frequencies well below a few kilohertz, however, may at first sight be surprising. Indeed, from the approximate relation

$$\omega_0^2 \simeq \frac{3P_0}{a^2\rho} \tag{1}$$

relating the bubble radius a to its natural frequency $\nu_0 = \omega_0/2\pi$, one finds, for example, $\nu_0 \simeq 2.8$ kHz for a bubble having the radius of 1 mm in water (density $\rho \simeq 1$ g/cm^3) at normal ambient pressure ($P_0 \simeq 1$ atm). However, bubbles in a cloud are in effect coupled oscillators, and one can therefore expect the existence of *normal modes* of the cloud itself at a substantially lower frequency than that of the individual constituent bubbles. An alternative argument leading to the same conclusion may be based on the observation that the speed of sound in a bubbly mixture can be an order of magnitude smaller than in the pure liquid, even at gas-volume fractions less than 1%. Therefore, to a first approximation, a region of bubbly liquid can be considered as enclosed by a rigid boundary and will then possess normal modes. However, the fact that the boundary is not really rigid has the consequence that the acoustic energy "trapped" in the bubbly region will leak out into the pure liquid.

The frequencies ω_k of these normal modes are readily estimated as follows [7]. Let the cloud have linear dimensions of order L. Then, from the analogy with similar systems [8], one expects eigenfrequencies of the order of $\omega_k \simeq kc_m/2L$, $k = 1, 2, \cdots$, where c_m is the effective speed of sound in the bubbly mixture given approximately by the well-known expression [9]–[11]:

$$c_m^2 \simeq \frac{P_0}{\rho\beta} \tag{2}$$

where β is the gas-volume fraction. If the constituent bubbles have a radius of order a, the gas-volume fraction may be estimated by $\beta \sim (a^3/L^3)N$, where N is the number of bubbles in the cloud. In this way we find:

$$\frac{\omega_k}{\omega_0} \sim \frac{k}{\beta^{1/6}N^{1/3}}. \tag{3}$$

The volume fraction here is raised to such a low power that the result is nearly independent of this variable. Hence all the frequencies, and in particular the lowest one corresponding to $k = 1$, are predicted to decrease essentially as the cube root of the bubble number. For $N \sim 1000$, the frequency reduction with respect to the single-bubble case would be of one order of magnitude [7].

The preceding estimate can be put on a firmer ground by means of a model of a bubbly liquid which is adequate up to gas-volume fractions of a few percent. The model, which regards the gas–liquid mixture as a continuum governed by effective equations, is essentially due to Foldy [12], and has been rederived by many others, in particular in [13]. Its predictions have been compared with experiment, most recently in [14], and a very good agreement was found. For completeness we briefly present the linearized version of this model in the next section. A series of papers containing detailed applications of it to the generation and scattering of sound by bubble clouds of different shape and in a number of situations is being prepared. The present study is a survey of the results on the generation of noise contained in these papers.

II. Mathematical Formulation

The averaged continuity and momentum equations applicable to a bubbly liquid at small gas-volume fraction may be

Manuscript revised May 1, 1990. This work was supported by the Ocean Acoustics Program of the Office of Naval Research.

N. Q. Lu and A. Prosperetti are with the Department of Mechanical Engineering, The Johns Hopkins University, 128 Latrobe Hall, Baltimore, MD 21218.

S. W. Yoon is with the Department of Physics, Sung Kyun Kwan University, Suwon 440-746, Korea.

IEEE Log Number 9036960.

written (see, e.g., [14, and references therein]):

$$\frac{1}{\rho c^2}\frac{\partial P}{\partial t} + \nabla \cdot \boldsymbol{u} = \frac{\partial \beta}{\partial t} \tag{4}$$

$$\rho\frac{\partial \boldsymbol{u}}{\partial t} + \nabla P = 0 \tag{5}$$

where $\boldsymbol{u}$ and P denote the average local center-of-mass velocity and pressure fields in the mixture, and c is the speed of sound in the pure liquid. In the present study, for simplicity, we assume the bubbles to have all the same equilibrium radius, and therefore the instantaneous gas volume fraction β is given by

$$\beta(\boldsymbol{x}, t) = \frac{4}{3}\pi n R^3(\boldsymbol{x}, t) \tag{6}$$

where n denotes the number of bubbles per unit volume, which can be taken to be a constant at small β [13]. Here $R(\boldsymbol{x}, t)$ denotes the instantaneous radius at position $\boldsymbol{x}$ and time t of a bubble having the equilibrium radius a.

Since in this study we shall confine ourselves to linear waves, there is no need to give in full detail the nonlinear formulation of a bubble response model that can be found in [14]. Let us simply set,

$$R = a(1 + X) \tag{7}$$

and note that, as shown in [15], for a time dependence proportional to exp $i\omega t$, the internal pressure p has the form:

$$p = p_e(1 - \Phi X) \tag{8}$$

where p_e is the equilibrium value

$$p_e = P_0 + \frac{2\sigma}{a} \tag{9}$$

with σ the surface tension, and

$$\Phi = \frac{3\gamma}{1 - 3(\gamma - 1)i\chi\left[(i/\chi)^{1/2}\coth(i/\chi)^{1/2} - 1\right]} \tag{10}$$

with γ the ratio of specific heats and

$$\chi = \frac{D}{\omega a^2} \tag{11}$$

in which D is the thermal diffusivity of the gas. With these results, it can be shown [14], [15] that the response of the bubbles to a harmonically oscillating average pressure field is given by

$$X = -\frac{(P - P_0)/\rho a^2}{\omega_0^2 - \omega^2 + 2ib\omega} \tag{12}$$

where P_0 is the undisturbed static pressure in the medium, and the natural frequency of the bubble ω_0 and effective damping constant b are given by

$$\omega_0^2 = \frac{p_e}{\rho a^2}\left(\mathrm{Re}\,\Phi - \frac{2\sigma}{a p_e}\right) \tag{13}$$

$$b = \frac{2\mu}{\rho a^2} + \frac{p_e}{2\rho\omega a^2}\,\mathrm{Im}\,\Phi + \frac{\omega^2 a}{2c}. \tag{14}$$

If the effect of surface tension is disregarded and the low-frequency result Re $\Phi \simeq 3$ is used, (13) reduces to the result (1) quoted before. As for the damping constant b, its three contributions arise from viscosity, heat transfer, and acoustic radiation, respectively.

Upon elimination of the velocity field between (4) and (5), use of (6) and (12), and linearization, we find the following effective wave equation valid for a time dependence proportional to exp $i\omega t$:

$$\nabla^2 P + k_m^2(P - P_0) = 0 \tag{15}$$

where k_m is the effective wave number in the mixture given by the dispersion relation,

$$k_m^2 = \frac{\omega^2}{c^2} + 4\pi\omega^2\frac{na}{\omega_0^2 - \omega^2 + 2ib\omega}. \tag{16}$$

The effective speed of sound in the mixture $c_m = \omega/k_m$ is given by

$$\frac{c^2}{c_m^2} = 1 + \frac{4\pi c^2 na}{\omega_0^2 - \omega^2 + 2ib\omega}. \tag{17}$$

The second term in the right-hand side is usually much larger than 1. With this approximation, and noting that at low frequencies the denominator can be approximated simply by ω_0^2 if (1) is used for this quantity, the result (2) previously quoted is recovered.

We show in Fig. 1 a graph of the phase velocity V of the waves as predicted by (17) as a function of the frequency ν in water at 1 bar pressure for bubbles with equilibrium radii of 0.1, 1, and 3 mm. (It should be noted that, upon writing $c/c_m = u - iv$, the actual phase velocity of the waves is given by c/u, rather than Re c_m.) The low-frequency limit is essentially given by (2), with the slight differences due to deviations from perfectly isothermal conditions. The high-frequency limit is the speed of sound in pure water, approximately 1500 m/s. The rapid dips in the curves occur near the resonance frequencies of the bubbles equal, from (13), to 31.6, 3.24, and 1.09 kHz, respectively. In general appearance, these results are very reminiscent of those for the dielectric constant of materials in the neighborhood of the region of anomalous dispersion and arise, of course, from similar physical reasons [16].

The fact that both the expressions for k_m and c_m are complex indicates that the propagation of sound in the mixture is accompanied by an exponential attenuation. The energy lost by the wave is used to overcome the viscous and thermal dissipation affecting the oscillation of the individual bubbles as described by the first and second terms of (14) for b. However, as described by the last term of (14), each bubble is also a scatterer of sound. Contrary to the other two, this mechanism does not lead to a dissipation of the acoustic energy into heat, but merely to the transformation of part of the acoustic energy contained in the coherent field into acoustic energy of the incoherent field.

In the situations modeled in the following, we shall assume that the bubbly mixture is separated from the pure liquid by geometric surfaces. Suitable continuity conditions at these

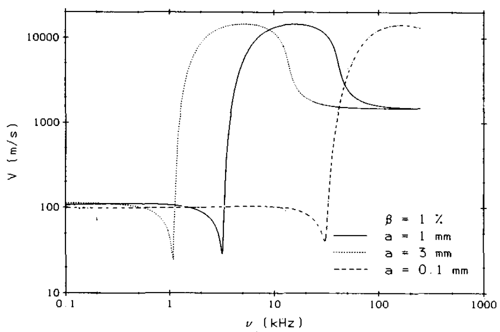

Fig. 1. Phase speed of pressure waves in bubbly water containing 1% air concentration by volume as a function of the waves' frequency. The dotted line is for a bubble radius $a = 3$ mm (with a corresponding natural frequency of 1.087 kHz), the solid line for $a = 1$ mm (3.24 kHz), and the dashed line for $a = 0.1$ mm (31.55 kHz).

surfaces have been given in [14] and [17]. Here we shall just quote those results. If the superscript "0" denotes quantities pertaining to the pure liquid, we shall require that

$$\boldsymbol{u} \cdot \boldsymbol{n} = \boldsymbol{u}^0 \cdot \boldsymbol{n} \tag{18}$$

$$P^0 = P \tag{19}$$

where $\boldsymbol{n}$ is the unit normal to the interface. These two relations derive from the requirements of conservation of mass and momentum across the interface to the same first order in β at which the averaged field equations (4) and (5) are valid. A more convenient formulation of (18), valid in the present time-harmonic case, can be obtained from (5), and is

$$\nabla P \cdot \boldsymbol{n} = \nabla P^0 \cdot \boldsymbol{n}. \tag{20}$$

III. Bubble Layers

The simplest case is that of a layer of bubbly liquid bounded by two infinite planes a distance L apart and parallel to the (y, z) plane. By restricting our attention to pressure waves propagating only in the x direction, we are thus dealing with effectively one-dimensional situations. We consider two cases: A screen in an infinite liquid, and a screen adjacent to a pressure-release surface. In the ocean, the first situation would model, for example, the bubbles transported downward by descending Langmuir currents [2]. The second case would instead correspond to the bubbly layer that nearly permanently covers the ocean surface [1]. We take the bubbly liquid to occupy the region $0 < x < L$, with the liquid extending to infinity in the positive x-direction. In the mixture region, the solution of the effective wave equation (15) is

$$P = P_0 + B_1 \sin(k_m x) + B_2 \cos(k_m x). \tag{21}$$

Since we are considering the normal-mode situation in which the acoustic source is the screen, we need only be concerned with outgoing waves, and therefore the solution in the pure liquid to the right $(x > L)$ of the screen is

$$P_+^0 = P_0 + A_1 \exp[-ik(x - L)] \tag{22}$$

where $k = \omega/c$ is the wave number in the pure liquid.

For the first case of a layer in an infinite liquid, the region $-\infty < x < 0$ is also occupied by pure liquid and, here, outgoing waves have the form:

$$P_-^0 = P_0 + A_2 \exp[ikx]. \tag{23}$$

Upon application of the boundary conditions (19) and (20) to (21)–(23), one finds a linear homogeneous system that admits two classes of solutions. Modes of oscillations with a pressure distribution symmetric about the screen's midplane have the characteristic equation,

$$\cos(k_m L/2) + i\frac{k_m}{k} \sin(k_m L/2) = 0. \tag{24}$$

Antisymmetric modes have instead the characteristic equation,

$$\cos(k_m L/2) + i\frac{k}{k_m} \sin(k_m L/2) = 0. \tag{25}$$

For the case of a bubbly layer adjacent to the free surface, the plane $x = 0$ is a pressure-release surface, and the boundary conditions (19) and (20) must be applied only at $x = L$, while at $x = 0$ we simply impose,

$$P = P_0. \tag{26}$$

In this way we are led to the characteristic equation:

$$\cos(k_m L) + i\frac{k}{k_m} \sin(k_m L) = 0. \tag{27}$$

It is clear that this solution corresponds to the odd one of the previous case for a screen twice as thick, as could have been anticipated, and need not be considered specifically.

Equations (24) and (25) are to be solved for the complex eigenfrequencies,

$$\omega = 2\pi\nu + i\alpha \tag{28}$$

of the oscillations of the bubbly layer. The task is far from trivial in view of the complexity of the roots, and it has been accomplished by a preliminary analysis based on the Nyquist criterion later refined by a secant method. Reference [18] contains details of the technique. We present a number of results in Figs. 2 to 7.

In Fig. 2 we show the real part ν of the eigenfrequencies of the first four normal modes as a function of the gas-volume fraction β. Odd-numbered modes are obtained from (25), and even-numbered ones from (24). The layer thickness is 0.1 m and the bubble radius 1 mm. Each bubble in isolation would have a frequency of 3.24 kHz, but it is obvious from the figure that the collective effects lead to dramatically smaller frequencies for the cloud as a whole. The imaginary part α of the eigenfrequencies (i.e., the decay rate) is plotted for the same case in Fig. 3.

To illustrate the effect of the bubble radius, we include in Fig. 4 a comparison of the first and third mode for bubbles having radii of 1 and 0.1 mm. For mode 1 the eigenfrequencies are away from resonance for both radii, and the results for the values of the radii are very close. For mode 3, however, the eigenfrequencies are close to the natural frequency of the 1-mm bubbles, and the corresponding large

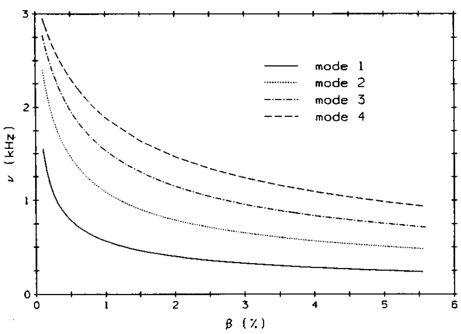

Fig. 2. The first four eigenfrequencies of a 0.1-m-thick bubbly layer in water according to equations (24) and (25) as a function of the air-volume fraction. The bubble radius is 1 mm.

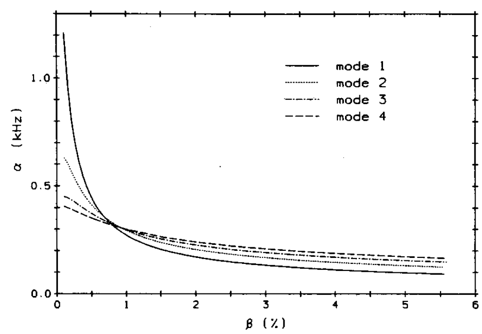

Fig. 3. Decay rate of the first four eigenmodes shown in the preceding figure as a function of the air-volume fraction.

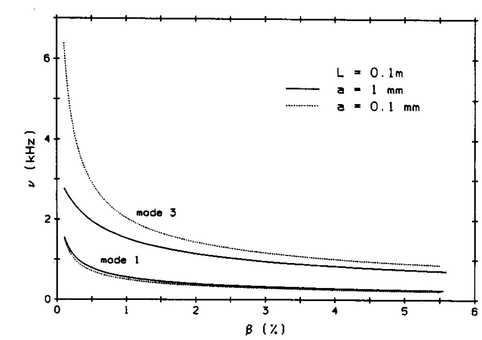

Fig. 4. Effect of the bubble radius on the eigenfrequencies of modes 1 and 3 for the case of the previous two figures.

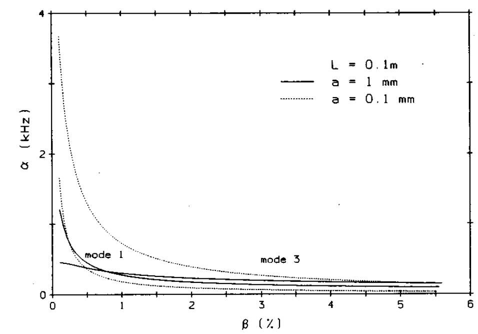

Fig. 5. Effect of the bubble radius on the decay rate of modes 1 and 3 for the case of Figs. 2 and 3.

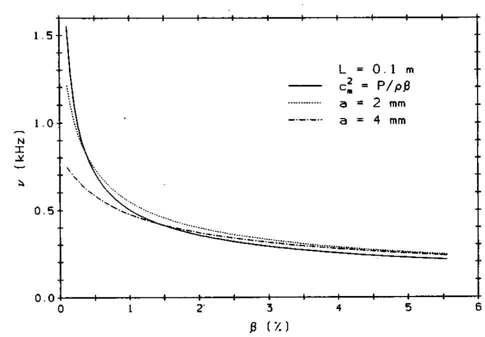

Fig. 6. The eigenfrequency of the lowest mode as predicted by the correct equation (17) for bubble radii of 2 and 4 mm, and by the simple approximation (2), for the case of Figs. 2 and 3.

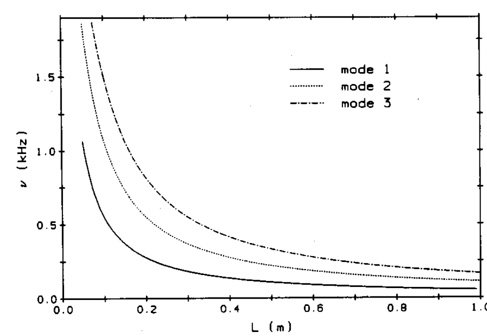

Fig. 7. Effect of the layer thickness on the eigenfrequency of the first three modes for an air-volume fraction of 1%.

effect on the phase velocity visible in Fig. 1 is reflected in the large difference between the two results. A similar picture emerges from Fig. 5, showing the damping rate for the same cases. Fig. 6 compares the results given by use of the correct expression (17) for c_m for the case of bubbles with radii of 2 and 4 mm (resonance frequencies of 1.63 and 0.816 kHz, respectively) with those obtained from the simple approximation (2). The results are in close agreement at the larger values of β, where the eigenfrequencies are small, but differ markedly for $\beta \rightarrow 0$. Finally, in Fig. 7, we show the effect of the layer's thickness on the first three eigenmodes, again for $\beta = 1\%$ and $a = 1$ mm. The very rapid decrease is quite striking and extends well into the region of oceanic ambient noise dominated by shipping [19].

IV. Surface Cloud

Another situation that is readily amenable to analysis is the case of a hemispherical cloud of radius R_c at a pressure-release plane surface. In an oceanic environment, this may be regarded as a very simple model of the bubble plume generated by an isolated wave-breaking event, and is therefore of particular relevance to the problem of underwater-noise generation. Since the problem is linear we can consider the different modes separately, and we therefore write the solution of the Helmholtz equation (15) inside the plume in the form:

$$P(r,\theta,\phi) = B_{ln} j_l(k_m r) Y_{ln}(\theta,\phi) \tag{29}$$

where the requirement of vanishing pressure on the plane $\theta = \frac{1}{2}\pi$ requires that $l + n$ be odd. A suitable form for the pressure field in the surrounding pure liquid is

$$P^0(r,\theta,\phi) = A_{ln} h_l^{(2)}(kr) Y_{ln}(\theta,\phi). \tag{30}$$

The imposition of the interface conditions (19) and (20) at $r = R_c$ gives the characteristic equation,

$$x\frac{j_{l-1}(x)}{j_l(x)} = s\frac{h_{l-1}^{(2)}(s)}{h_l^{(2)}(s)} \tag{31}$$

where $x = k_m R_c$ and $s = kR_c$. This equation is solved numerically in the same way as in the previous case.

To illustrate these results, we study only axisymmetric modes for which $n = 0$, and are therefore forced to consider odd values of l. Figs. 8 and 9 show the eigenfrequency and the decay rate for the modes $l = 1, 3, 5$ as a function of the gas-volume fraction for a cloud radius of 1 m and bubbles of 1-mm radius. Again, the very low frequencies of oscillation predicted by these results are quite striking. The following figure shows the damping rates defined by (28). The effect of the cloud radius on the $l = 1$ mode, both real and imaginary parts, is shown in the Figs. 10 and 11. The scaling (3) is very well supported by these results.

V. Cylindrical Cloud

We now turn to the case in which the bubble cloud is bounded by a cylindrical surface of radius R_c. From the point of view of oceanic noise sources, such a configuration looks rather artificial. Our only reason for addressing it here is the fact that some recent experiments have been conducted with this geometry [20], so that a comparison with the theoretical predictions is possible.

Again we consider the different modes separately and write the solution of the Helmholtz equation (15) in the bubbly region in the form:

$$P = B_n J_n\left(r\sqrt{k_m^2 - \kappa^2}\right) e^{i\kappa z} e^{in\theta}. \tag{32}$$

To simulate the experimental situation to be described shortly, we take the surrounding pure-liquid region to be bounded by a rigid concentric circular wall of radius R_f, on which the condition,

$$\boldsymbol{u}^0 \cdot \boldsymbol{n} = 0 \tag{33}$$

must be imposed. The solution in the pure liquid may be written as

$$P^0 = A_n\left[H_n^{(2)}\left(r\sqrt{k^2-\kappa^2}\right) - \tilde{H} H_n^{(1)}\left(r\sqrt{k^2-\kappa^2}\right)\right] e^{i\kappa z} e^{in\theta} \tag{34}$$

where

$$\tilde{H} = \frac{H_n^{(2)\prime}\left(\sqrt{k^2-\kappa^2}\,R_f\right)}{H_n^{(1)\prime}\left(\sqrt{k^2-\kappa^2}\,R_f\right)}. \tag{35}$$

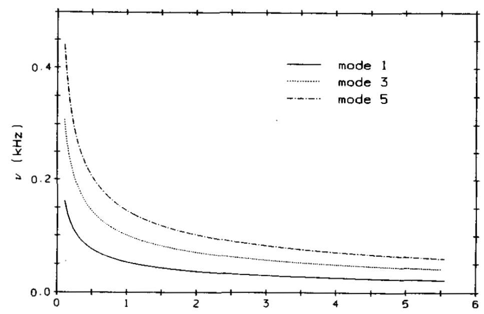

Fig. 8. The first three eigenfrequencies of a 1-m-radius hemispherical bubble cloud at the water surface according to equation (31) as a function of the air-volume fraction. The bubble radius is 1 mm.

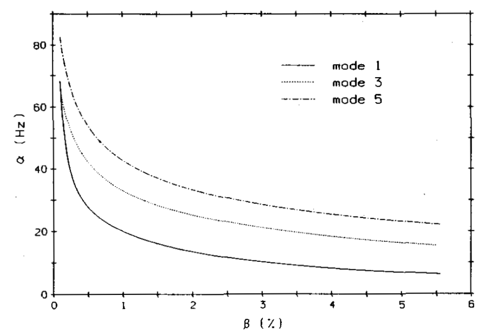

Fig. 9. Decay rate of the first three eigenmodes shown in the preceding figure as a function of the air-volume fraction.

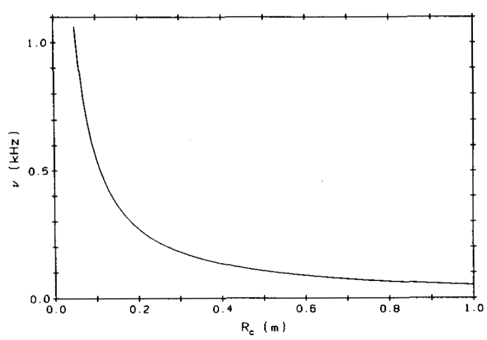

Fig. 10. Effect of the cloud radius R_c on the frequency of the lowest eigenmode of the hemispherical cloud considered in the previous two figures. The air-volume fraction is 1%.

Upon imposing the interface conditions (19) and (20) at R_c, we then find the characteristic equation:

$$x\frac{J_{n-1}(x)}{J_n(x)} = s\frac{\dfrac{H_{n-1}^{(2)}(s)}{H_n^{(2)}(s)} - \tilde{K}\dfrac{H_{n-1}^{(1)}(s)}{H_n^{(1)}(s)}}{1 - \tilde{K}} \tag{36}$$

with

$$x = \sqrt{k_m^2 - \kappa^2}\,R_c$$
$$s = \sqrt{k^2 - \kappa^2}\,R_c$$

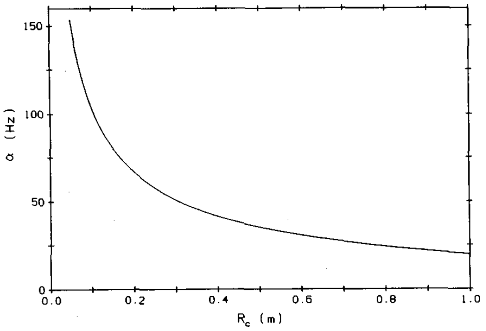

Fig. 11. Effect of the cloud radius R_c on the damping of the lowest eigenmode of the hemispherical cloud considered in Figs. 8 and 9. The air-volume fraction is 1%.

$$y = \sqrt{k^2 - \kappa^2}\, R_f$$

and

$$\tilde{K} = \frac{\dfrac{H_{n-1}^{(2)}(y)}{H_n^{(2)}(y)} - \dfrac{n}{y}}{\dfrac{H_{n-1}^{(1)}(y)}{H_n^{(1)}(y)} - \dfrac{n}{y}} \, \frac{H_n^{(1)}(s)}{H_n^{(2)}(s)} \, \frac{H_n^{(2)}(y)}{H_n^{(1)}(y)}. \tag{37}$$

These equations can be somewhat simplified in the case of $n = 0$, in which they become:

$$x \frac{J_1(x)}{J_0(x)} = s \frac{\dfrac{H_1^{(2)}(s)}{H_0^{(2)}(s)} - \tilde{K} \dfrac{H_1^{(1)}(s)}{H_0^{(1)}(s)}}{1 - \tilde{K}} \tag{38}$$

and

$$\tilde{K} = \frac{H_1^{(2)}(y)}{H_1^{(1)}(y)} \, \frac{H_0^{(1)}(s)}{H_0^{(2)}(s)}. \tag{39}$$

Details of the experiment will be published elsewhere [20]; a brief summary is adequate here. The data were taken in a square tank with sides of 1 m. A circular bank of hypodermic needles was placed in the center of the tank, with the tip of the needles at a depth h below the free surface. High-pressure air was fed through the needles, and different gas-volume concentrations in the resulting bubble column were obtained by varying the air flow rate. The bubble radius was in the range of 1.5–2.5 mm. The underwater sound in the tank was recorded with a hydrophone and was Fourier-analyzed. The spectrum always contained a prominent low-frequency peak, which is interpreted as being due to the self-induced oscillations of the bubble column. Measurement of the mode shape in the vertical z-direction shows a pressure profile very close to a sinusoidal half-wave, and accordingly we shall take $\kappa = \pi/h$ in (38).

Fig. 12 shows a comparison between the lowest mode predicted by (38) and the measured results for bubble columns of three different radii—70, 54, and 46 mm. Here the bubble radius has been taken to be 1.5 mm, and the "equivalent" cylindrical tank radius $R_f = 0.75$ m. As shown in Fig. 13, in which the effect of R_f is illustrated, and in Fig. 14, which indicates the dependence of the results on the bubble radius, both quantities have a negligible effect on the results. Therefore it may be fairly stated that the exceptionally favorable comparison of theory and data in Fig. 12 involves no adjustable parameter. Such a result is extremely gratifying and lends considerable support to the validity of the theory described in this paper.

The decay rate of the oscillations is, as in the previous case, in the range of a few tens of s^{-1}. The corresponding decay time is relatively short, but the prominence with which

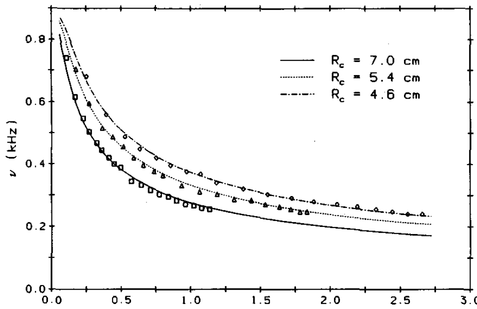

Fig. 12. Measured values of the lowest eigenfrequencies of a cylindrical bubble cloud compared with theory, equation (38). The squares and the continuous line are for a cloud radius $R_c = 70$ mm, the triangles and the dotted line for $R_c = 54$ mm, and the diamonds and dash-and-dot line for $R_c = 46$ mm. Column height $h = 0.82$ m.

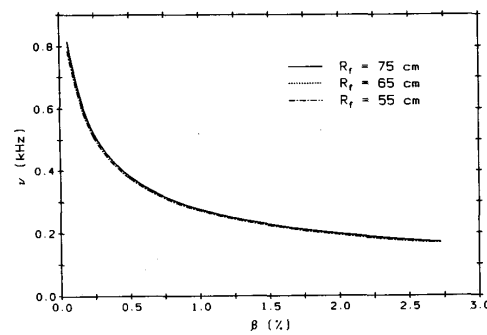

Fig. 13. Effect of the tank radius on the results of the previous figure for $R_c = 70$ m, $a = 1.5$ mm, and $h = 0.82$ m.

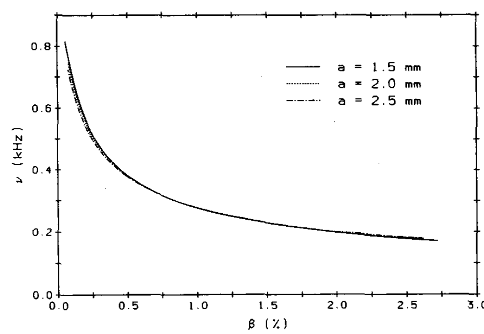

Fig. 14. Effect of the bubble radius on the results of Fig. 12 for $R_f = 0.75$ m, $R_c = 70$ mm, and $h = 0.82$ m.

the peak appeared in the Fourier transform of the recorded signal indicates that the oscillations were relatively energetic. This may be somewhat unexpected, because the only source of energy in the system was the process of bubble detachment from the needles and the upward motion of the bubbles. This circumstance suggests that cloud resonances are easily excited and that an appreciable amount of noise is likely to be emitted by the clouds produced by such energetic events as wave breaking.

VI. Conclusions

We have presented an analysis of the oscillations of bubble clouds of simple geometrical shapes. In one case for which data are available, the predictions of the theory agree remarkably well with experiment. Qualitatively, the most important conclusion which can be drawn from our analysis is the existence of collective modes of oscillation of the clouds one or two orders of magnitude below the natural frequency of the constituent bubbles. This is the range below 1 kHz where considerable wind dependence of oceanic ambient noise is found [19], [21].

Before the hypothesis that these bubble clouds contribute significantly to oceanic ambient noise can be unambiguously proven, it is necessary to study in detail the manner in which these clouds are energized, the spectrum and intensity of the acoustic emission from real wave-breaking events, the bubble content of the plume, etc. This is clearly a major experimental task. Our objective here was simply to show that the possibility is a real one, and is compatible with the limited data presently available.

References

[1] S. A. Thorpe, "On the clouds of bubbles formed by breaking wind-waves in deep water, and their role in air-sea gas transfer," *Phil. Trans. Roy. Soc. London*, vol. A304, pp. 155-210, 1982.

[2] S. A. Thorpe, "The effect of Langmuir circulation on the distribution of submerged bubbles caused by breaking wind waves," *J. Fluid Mech.*, vol. 142, pp. 151-170, 1984.

[3] W. M. Carey, "Low-frequency ocean surface noise sources," *J. Acoust. Soc. Amer.*, vol. 78, nos. S1-S2, 1985.

[4] A. Prosperetti, "Bubble-related ambient noise in the ocean," *J. Acoust. Soc. Amer.*, vol. 78, no. S2, 1985.

[5] A. Prosperetti, "Bubble dynamics in oceanic ambient noise," in *Sea Surface Sound*, B. R. Kerman, Ed. Boston: Kluwer, 1988, pp. 151-171.

[6] W. M. Carey and D. Browning, "Low-frequency ocean ambient noise: Measurements and theory," in *Sea Surface Sound*, B. R. Kerman, Ed. Boston: Kluwer, 1988, pp. 361-376.

[7] A. Prosperetti, "Bubble-related ambient noise in the ocean," *J. Acoust. Soc. Amer.*, vol. 84, pp. 1042-1054, 1988.

[8] L. Landau and E. Lifshitz, *Fluid Mechanics*. New York: Pergamon, 1959.

[9] A. B. Wood, *A Textbook of Sound*. London: Bell & Sons, 1932, pp. 360-364.

[10] L. van Wijngaarden, "One-dimensional flow of liquids containing small gas bubbles," *Ann. Rev. Fluid Mech.*, vol. 4, pp. 369-396, 1972.

[11] D. G. Crighton and J. E. Ffowcs-Williams, "Sound generated by turbulent two-phase flows," *J. Fluid Mech.*, vol. 36, pp. 585-603, 1969.

[12] L. L. Foldy, "The multiple scattering of waves," *Phys. Rev.*, vol. 67, pp. 107-119, 1945.

[13] R. E. Caflisch, M. J. Miksis, G. C. Papanicolaou, and L. Ting, "Effective equations for wave propagation in bubbly liquids," *J. Fluid Mech.*, vol. 153, pp. 259-273, 1985.

[14] K. W. Commander and A. Prosperetti, "Linear pressure waves in bubbly liquids: Comparison between theory and experiments," *J. Acoust. Soc. Amer.*, vol. 85, pp. 732-746, 1989.

[15] A. Prosperetti, L. A. Crum, and K. W. Commander, "Nonlinear bubble dynamics," *J. Acoust. Soc. Amer.*, vol. 83, pp. 502-514, 1988.

[16] J. D. Jackson, *Classical Electrodynamics*. New York: Wiley, 1975.

[17] E. L. Carstensen and L. L. Foldy, "Propagation of sound through a liquid containing bubbles," *J. Acoust. Soc. Amer.*, vol. 19, pp. 481-501, 1947.

[18] N. Q. Lu and A. Prosperetti, "Acoustics of bubble layers," *J. Acoust. Soc. Amer.*, to be published.

[19] G. M. Wenz, "Acoustic ambient noise in the ocean: Spectra and sources," *J. Acoust. Soc. Amer.*, vol. 34, pp. 1936-1956, 1962.

[20] S. W. Yoon, L. A. Crum, A. Prosperetti, and N. Q. Lu, "Experimental investigation of the collective oscillations of a bubble cloud," *J. Acoust. Soc. Amer.*, to be published.

[21] P. C. Wille and D. Geyer, "Measurements on the origin of the wind dependent ambient noise variability in shallow water," *J. Acoust. Soc. Amer.*, vol. 75, pp. 173-185, 1984.

★

Nan Q. Lu received the B.S. degree in mechanical engineering from the City College of New York, and the M.S. degree in mechanical engineering from the Johns Hopkins University, Baltimore. She is currently working on her Ph.D. dissertation, entitled "Bubble Clouds as Sources and Scatterers of Underwater Sound," which she expects to complete by October 1990. She has authored four papers.

Ms. Lu is a member of Tau Beta Pi.

★

Andrea Prosperetti obtained the Laurea in Fisica at the University of Milano, Italy, and the doctorate degree in engineering science from the California Institute of Technology, Pasadena.

During the period between 1975 and 1985 he was Assistant, then Associate Professor of Physics at the University of Milan. In 1985 he became Professor at the Johns Hopkins University, Baltimore, where he is currently the Chairman of the Department of Mechanical Engineering. His principal interests are in bubble dynamics, free-surface flows, multiphase flows, and numerical methods.

Dr. Prosperetti is a Fellow of the Acoustical Society of America.

★

Suk Wang Yoon (SM'89) obtained the Ph.D. degree in physical acoustics from the University of Texas at Austin.

He was Assistant Professor of Physics at Sung Kyun Kwan University between 1985 and 1989, after which he was promoted to Associate Professor, then Department Chairman. The work reported here was carried out while he was on leave at the National Center for Physical Acoustics at the University of Mississippi, Oxford, supported by the Korea Science and Engineering Foundation Fellowship.

Dr. Yoon is a member of the Acoustical Society of America.